Abdominal Radiology (2019) 44:3786–3799
https://doi.org/10.1007/s00261-019-02111-2

SPECIAL SECTION: UROTHELIAL DISEASE

CT urography: how to optimize the technique

Karen Cheng[1] · Fiona Cassidy[1] · Lejla Aganovic[1] · Michael Taddonio[1] · Noushin Vahdat[1,2]

Published online: 17 July 2019

Abstract

Purpose Computed tomography urography (CTU) has emerged as the modality of choice for imaging the urinary tract within the past few decades. It is a powerful tool that enables detailed anatomic evaluation of the urinary tract in order to identify primary urothelial malignancies, benign urinary tract conditions, and associated abdominopelvic pathologies. As such, there have been extensive efforts to optimize CTU protocol.

Methods This article reviews the published literature on CTU protocol optimization, including contrast bolus timing, dose reduction, reconstruction algorithms, and ancillary practices.

Conclusion There have been many advances in CTU techniques, which allow for imaging diagnosis of a wide spectrum of diseases while minimizing radiation dose and maximizing urinary tract distension and opacification.

Keywords CT urography · Technique · Dose reduction

Background

CT urography (CTU) has become the mainstay for the radiologic evaluation of urologic conditions within the past few decades. Initially utilized only for patients with risk factors for urothelial cancer, CTU is now recommended as the imaging study of choice for most adult patients with gross hematuria or persistent microhematuria as of the 2012 American Urological Association (AUA) guidelines [1] and the 2014 American College of Radiology (ACR) Appropriateness Criteria [2]. CTU has largely replaced its predecessor, intravenous urography (IVU), which had lower sensitivity for renal masses, did not allow for distinction of overlapping structures, and provided less anatomic detail [1, 3].

An estimated 4% of individuals undergoing work-up for asymptomatic hematuria will have an underlying urinary tract malignancy [1]. CTU, which allows for comprehensive evaluation of the kidneys and urothelial system, results in earlier diagnosis of both upper and lower tract urothelial cell carcinoma and renal cell carcinoma as compared to other imaging modalities such as ultrasound or IVU [4]. CTU also allows for the identification of other benign etiologies of hematuria, including calculi, trauma, benign prostatic enlargement, or infection, and likely reduces the number of tests required to diagnose the cause of hematuria [3].

CT urography

Technique

CTU refers to any CT examination of the urinary tract that includes post-contrast excretory phase imaging [3]. The primary goal of a CTU protocol is to obtain maximum distension and opacification of the upper tract collecting system, the ureters, and the urinary bladder in the excretory phase to increase sensitivity for detection of urothelial neoplasms. At the same time, the exam must also have sufficient sensitivity to detect a variety of other abnormalities that may cause hematuria, including renal calculi and renal cell carcinoma [5]. Since CT involves the use of ionizing radiation, a secondary goal in CTU protocol optimization is to reduce the necessary dose to achieve diagnostic images. The single bolus protocol is the most widely used technique with the second most commonly used protocol, the split bolus

✉ Noushin Vahdat
Noushin.Vahdat@gmail.com

[1] Department of Radiology, University of California, San Diego, 200 W. Arbor Drive, San Diego, CA 92103, USA

[2] Department of Radiology, VA Medical Center, San Diego, 3350 La Jolla Village Drive, Mail Code: 114, San Diego, CA 92161, USA

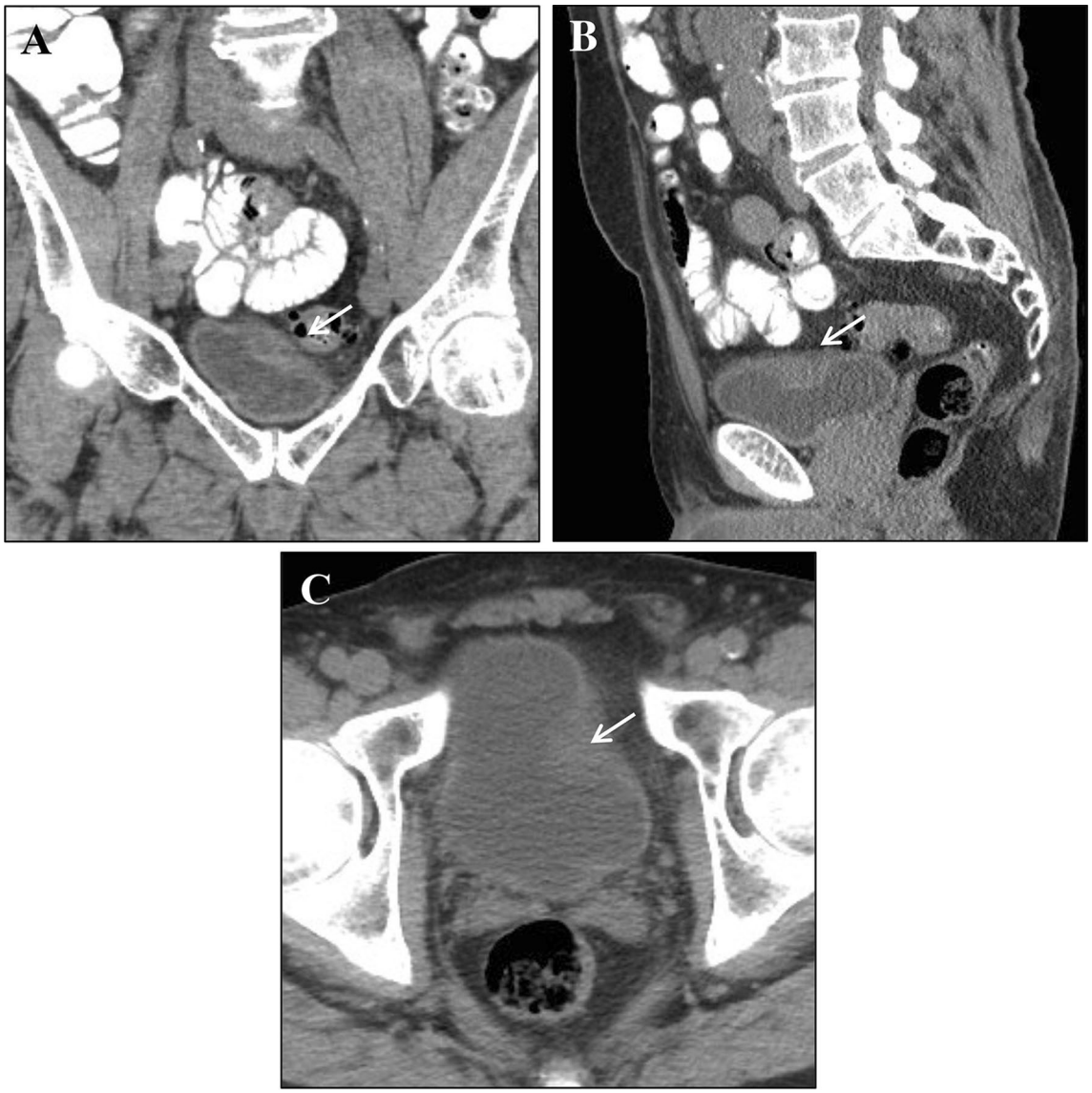

Fig. 1 Coronal and sagittal reformatting. Coronal (**a**) and sagittal (**b**) reformats of a non-contrast-enhanced exam clearly demonstrate a tumor (arrows) within the bladder dome, which could easily have been missed on axial images alone (**c**)

protocol, reserved for younger patients in order to minimize the radiation dose [3, 6].

Single bolus

The traditional technique for CTU is to acquire non-contrast images, administer the full contrast bolus and then acquire images in the nephrographic phase (80 to 120 s) and delayed excretory phase (5 to 15 min). Additional image acquisition in the corticomedullary phase (30 to 40 s) is optional and performed at some institutions. Following the image acquisitions, coronal and sagittal reformations are incorporated in most CTU protocols to increase sensitivity and visualization of the kidneys and urothelium (Fig. 1). This single bolus technique yields maximal opacification and distension of the urinary tract because the entire administered intravenous contrast volume contributes to the excretory phase [5, 6]. This is also the simplest technique for the technologist to perform, as it only requires a single contrast injection. However, since three or four separate acquisitions are performed, this technique results in the highest radiation dose [6].

Given the concern regarding radiation dose, there are divided opinions on whether the corticomedullary phase is necessary in a standard CTU, or whether three acquisition phases (non-contrast, nephrographic, and excretory) are sufficient. The reported advantages of the corticomedullary phase are that it provides more vascular and perfusion information than the nephrographic phase [7], allows for

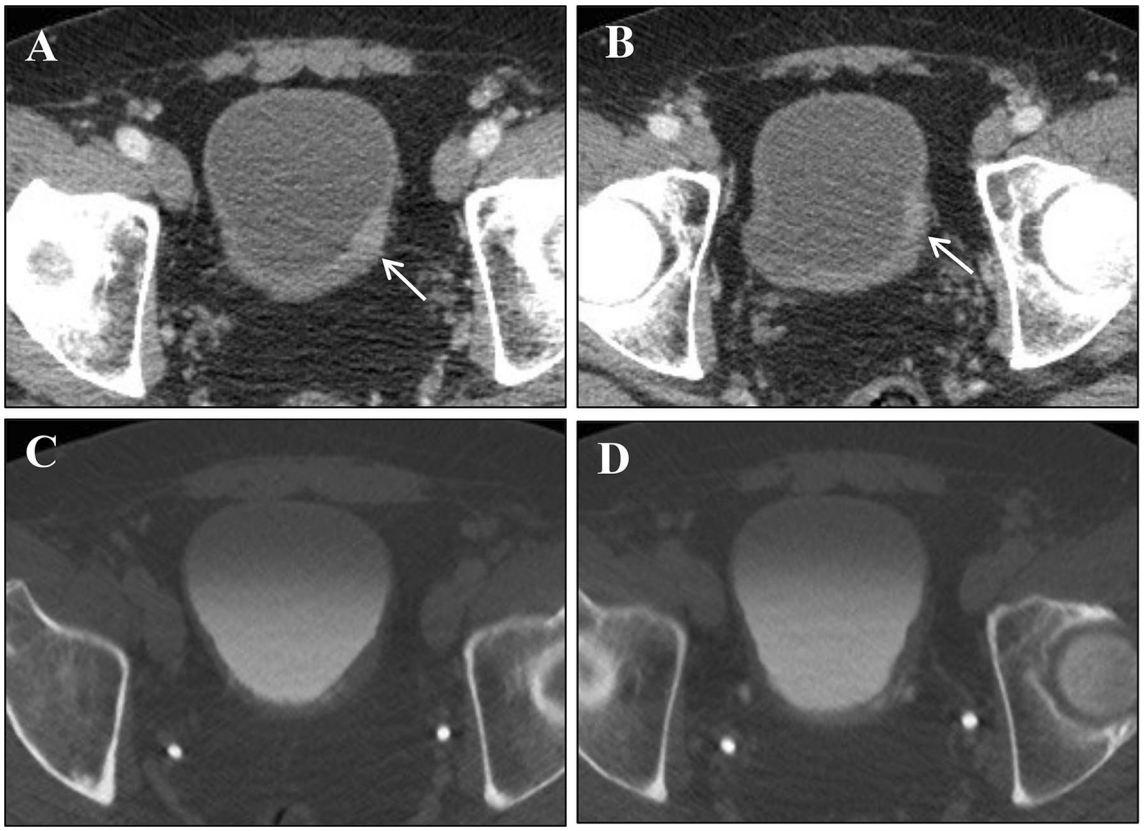

Fig. 2 Nephrographic phase tumor enhancement. Axial images in the nephrographic phase (**a**, **b**) demonstrate mucosal tumors (arrows) more effectively than do axial images through the same level of the mass during the excretory phase (**c**, **d**)

better characterization of renal cortical masses [8], and detection of hypervascular metastases. Additionally, it may have a higher sensitivity and negative predictive value for the detection of bladder tumors than either the nephrographic or excretory phases alone [9, 10]. Although the corticomedullary phase can occasionally increase the diagnostic yield of the examination, many radiology departments choose to omit this phase because the small added benefit does not justify the increased dose [11]. Accordingly, at our institution the corticomedullary phase is not performed; we obtain three acquisitions, beginning with non-contrast images to the level of the pelvic brim, after which we administer 120 mL of Iohexol (Omnipaque 350, GE Healthcare), followed by a bolus of 250 mL of normal saline. Post-contrast images through the abdomen and pelvis are then acquired during nephrographic phase (90 s) and excretory phase (10 min).

As the primary purpose of the nephrographic phase is the evaluation of renal parenchyma, one could also conceivably reduce dose by limiting the nephrographic phase images to the kidneys only. However, studies have shown that nephrographic phase images increase sensitivity for urothelial carcinoma [12] and, in the absence of a corticomedullary phase, bladder tumors demonstrate the most enhancement during nephrographic phase [10] (Fig. 2). Most institutions, therefore, include entire abdomen and pelvis on the nephrographic phase acquisition to optimize evaluation of the ureters and bladder. Extending the nephrographic phase imaging to include the pelvis also facilitates complete tumor staging and evaluation of associated findings [13].

Institutional protocols for the single bolus technique can vary not only in the number of acquisitions, but also in the timing of each acquisition phase, particularly for the nephrographic and delayed excretory phases. The nephrographic phase can be acquired between 80 and 120 s after the contrast injection [14]. Acquisition of images too early, before the cortex and medulla are uniformly opacified, can result in misinterpretation. For example, a non-opacified renal medulla may simulate a tumor [15]. In our experience, image acquisition at 100 s following contrast injection yields homogeneous opacification of the renal parenchyma. However, a small percentage of patients can already have early excretion of contrast into the collecting system, which can obscure evaluation of mucosal enhancement within the renal pelvis. Therefore, we have recently changed the nephrographic imaging time to 90 s post-contrast administration.

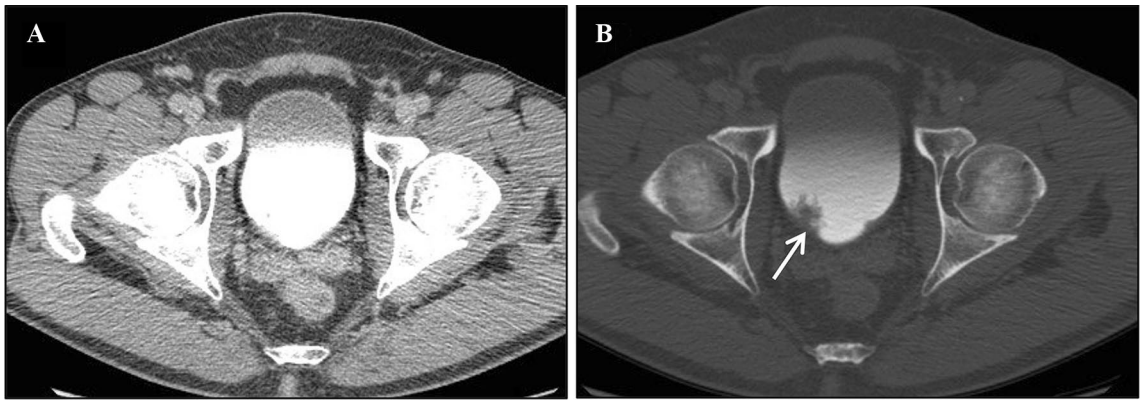

Fig. 3 Obscuration of tumor by dense contrast. Dense contrast within the bladder (**a**) on axial images in the excretory phase can obscure tumors. Appropriate windowing (**b**) of the same image can help improve detection of tumors (arrow)

The excretory phase begins at 3 min after the start of contrast injection [14] and timing delays of up to 15 min have been reported in the literature [16]. The variability in protocols likely reflects the broad range of normal excretory function, as each patient will have a different delay time at which their urinary tract is optimally opacified and distended, especially in the setting of impaired renal function. Some authors have proposed using single-slice, low-dose test images through the mid-ureter to individualize timing of the excretory phase imaging [17], but this increases the complexity of the protocol. In general, longer delay times of at least 10 min are recommended [13] to increase the likelihood that the distal ureter will be adequately opacified. However, waiting for an excessive time can increase the density of contrast within the ureters and bladder. Although appropriate windowing of images can help in certain cases (Fig. 3), resultant streak artifact can be a problem with extremely dense excreted contrast within the collecting system [18]. At our institution, we obtain the excretory phase images at 10 min following the single bolus injection to balance competing concerns of under-distension and excessive contrast density.

An additional urothelial phase has also been evaluated for the sensitivity of detecting urothelial tumors. This phase is acquired at 60-70 s following the administration of the contrast, an intermediate between the corticomedullary and nephrographic phases, and roughly the same time delay as a portal venous phase acquisition for the liver. This phase of imaging has been shown to have a high detection rate for upper tract urothelial lesions, with sensitivity and specificity of 95% and 97%, respectively [19]. The urothelial phase also has a higher sensitivity for the detection of bladder tumors than the excretory phase alone (89.3% vs. 70.5%) [20]. Although no study to date has specifically compared the urothelial phase alone to a more comprehensive CTU including an excretory phase or to the nephrographic phase as part of a multiphase protocol, combined nephrographic and excretory phases have been shown to be complementary in the detection of upper tract tumors [12], suggesting that both of these phases likely add value to the exam. We, therefore, do not utilize the urothelial phase at our institution. The urothelial phase has not yet been proven to be superior either to the nephrographic phase or the combined nephrographic and excretory phases if used alone, and the addition of the urothelial phase to the existing phases would result in unjustifiable increased radiation dose in the absence of data demonstrating a clear added benefit.

Split bolus

In the split bolus technique, as the name suggests, the contrast bolus is given in two separate injections. Following the non-contrast exam, part of the contrast is given. Optional corticomedullary images are obtained as a designated delay time elapses, then the second portion of the contrast, which is commonly larger than or equal amount to the first portion, is given at about 5 to 8 min from the first injection, and combined nephrographic–excretory phase images are acquired (Fig. 4). Much work has been done to determine the best allocation ratio of contrast between the first and second portions of the split bolus, as well as the optimal delay time, with some authors suggesting giving a larger bolus in the second injection to improve renal parenchymal enhancement and a delay time of 8 min from the first injection to maximize ureteral distension and opacification [21]. Split bolus technique is recommended in younger patients because it reduces the radiation dose. However, it is less sensitive for the detection of smaller renal cell carcinomas since fewer post-contrast phases are available and there may be streak artifact present from contrast in the collecting system [5]. Additionally, since only a part of the total contrast bolus

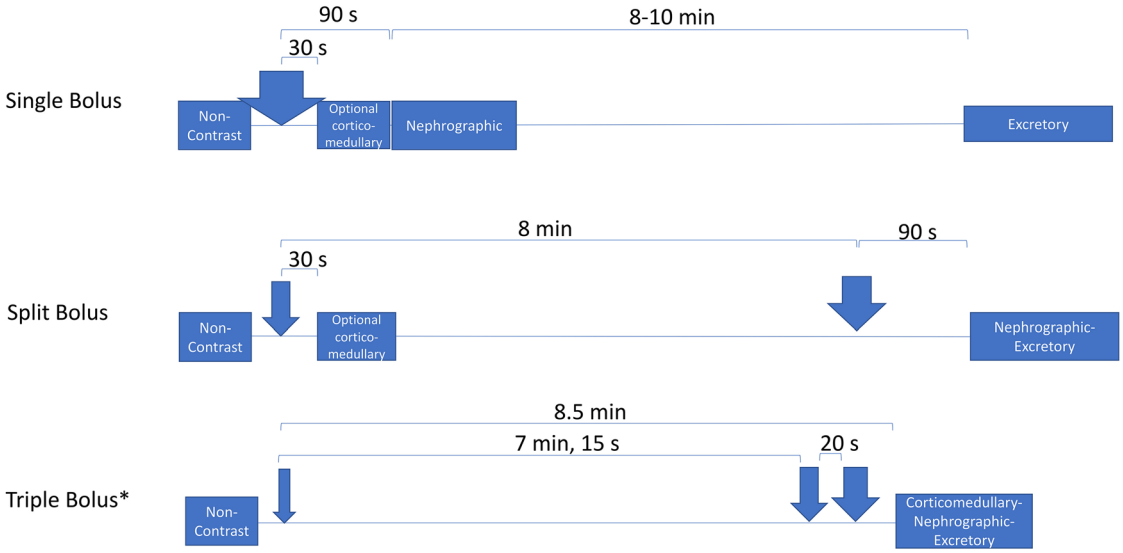

Fig. 4 Single, split, and triple bolus protocols. Schematic representation of the single, split, and triple bolus protocols with arrows indicating bolus injection. Thickness of the arrows indicate the amount and fraction of injected contrast

contributes to the excretory phase, this technique has poorer contrast opacification and distension of the urinary tract. Despite this limitation, split bolus CTU has been reported to have a similar sensitivity for upper tract urothelial carcinoma [6] as standard single bolus technique. One study reported a sensitivities and specificities of 100% and 99% for pathology-proven malignancies of the renal collecting system and ureter, and 74% and 100% for the malignancies of the urinary bladder, respectively [22].

We follow the split bolus protocol in patients less than 40 years of age (Fig. 5) as this population has been reported to have a low incidence of pathologies not detectable on unenhanced CT alone [3], likely due to the low pretest probability for urothelial malignancy [23]. Our protocol includes a non-contrast exam from the top of the kidneys through the pelvis, and a combined nephrographic–excretory phase to include the entire abdomen and pelvis. After the non-contrast scan, the intravenous contrast is divided into two separate doses with the initial dose of 50 mL Omnipaque 350 and 250 mL intravenous saline. This is followed by a second administration of 80 mL Omnipaque 350 about 8 min after the initial contrast dose. Subsequently, the combined nephrographic–excretory phase is performed at 90 s after the second contrast dose. We achieve significant dose reduction by only using two imaging phases and using lower mA (milliamperes) technique for these younger patients.

Triple bolus

The triple bolus technique, which is performed at only a few institutions, takes the principle of split bolus one step further, separating the total contrast volume into three injections (Fig. 4). Non-contrast images are acquired, then the first portion of the bolus is given, a delay time elapses, the second portion of the bolus is given, a delay time elapses, then the third portion of the bolus is given, and finally, post-contrast images are acquired. The resultant images are combined corticomedullary–nephrographic–excretory phase, which demonstrate enhancement of the arteries, renal parenchyma, and collecting system simultaneously. As with the split bolus technique, only a portion of the total contrast volume contributes to excretory imaging; therefore, there is decreased distention and opacification of the ureters. However, a study of 110 patients by Kekelidze et al. demonstrated complete opacification of the intrarenal collecting system in 91% of cases and complete opacification of the proximal ureter in 82% of cases, with non-opacification of the distal ureters and bladder in only 21% and 20% of cases, respectively [24]. For comparison, non-opacification of the distal ureters has been reported in 25–33% of cases for the single bolus triple-phase protocol, which should theoretically have the maximal ureteral opacification [25]. The Kekelidze et al. study also showed that the major advantage of triple bolus technique was a reduced radiation dose to 13.2 mSv as

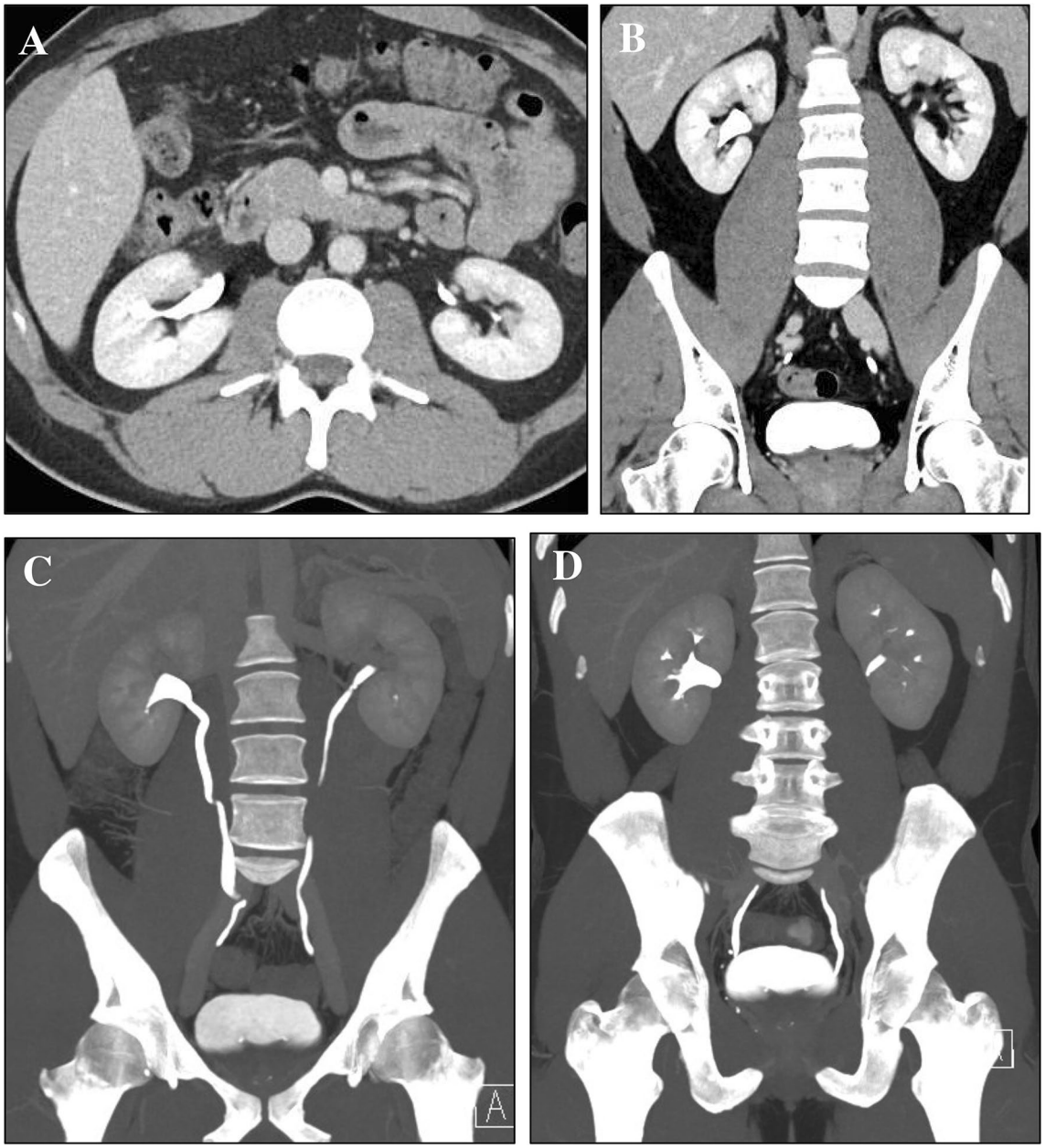

Fig. 5 Split Bolus Technique. Axial (**a**) and coronal reformats (**b**) from a 34-year-old patient who was imaged using the split bolus technique demonstrate uniform opacification of the renal parenchyma, as well as contrast within the urinary tract. The entire ureter is not seen on the same coronal slice, but most of the mid-ureter is opacified on the corresponding coronal MIP reconstruction (**c**), and the proximal and distal ureters are seen in a different slice of the MIP reconstruction (**d**)

compared to 23.4 mSv for the single bolus technique at the same institution [24].

3D reformats

Several different 3D reformation techniques can be utilized to enhance visualization of the urinary tract without increasing radiation exposure, including maximal intensity projection images (MIP), average intensity projection (AIP), volume-rendered reconstruction (VR), and curved planar reformats (CPR).

To generate MIP images, algorithms choose the highest attenuation voxels along lines in the 3D volumetric dataset and project them into a 2D image (Fig. 6). This technique highlights subtle sites of ureteral narrowing, abnormal urothelial thickening, and enhancement that can be easily missed on axial images alone [6]. However, the 2D representation may obscure 3D structural relationships. Additionally,

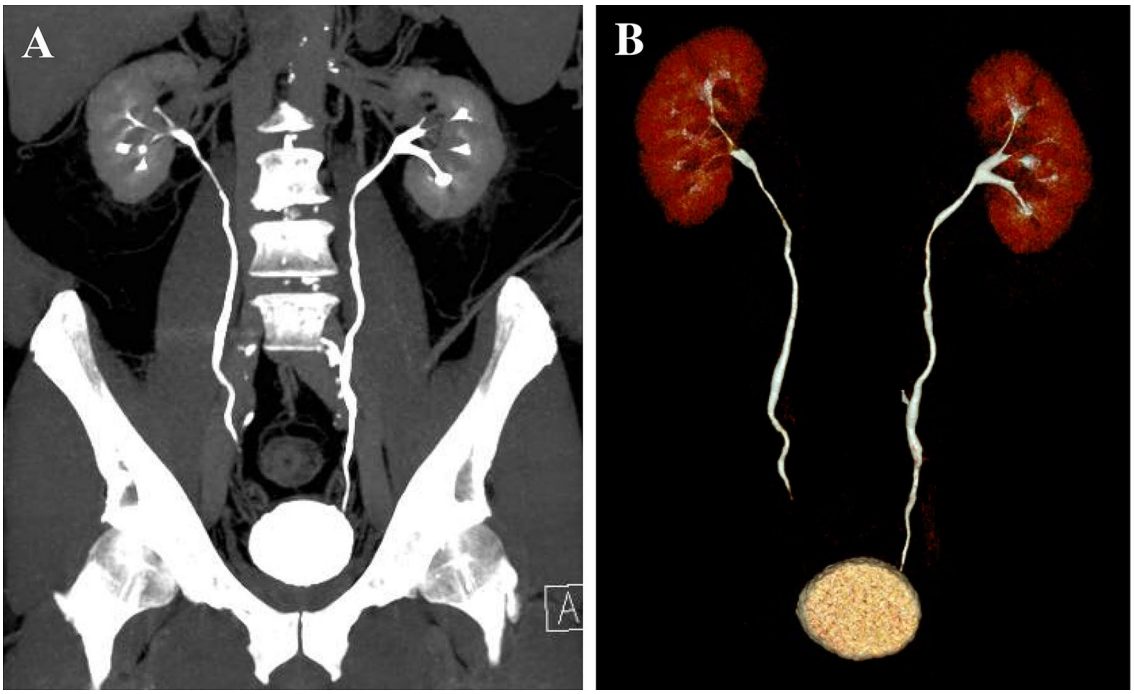

Fig. 6 3D Reformation Techniques. MIP image (**a**) and VR Reconstruction images (**b**) allow for improved visualization of the urinary tract

contrast-enhanced vessels and intrinsically high attenuation structures like calcifications adjacent to the ureters may be erroneously interpreted as excreted contrast by these algorithms, further complicating the evaluation.

AIP algorithms, on the other hand, choose the average attenuation along lines in the dataset to project onto a 2D image [26]. While AIP is useful for hollow structures like intestines, MIP tends to work better for contrast-material filled structures [26]. AIP summation can lead to loss of contrast resolution between the opacified collecting system and adjacent structures [27].

VR reconstructions are created by assigning a color and transparency to a particular voxel based on the specific tissue contents and attenuation of that voxel [6]. Like MIP images, VR images allow for improved visualization of subtle urothelial thickening [6]. However, it has the added advantages of maintaining 3D data and allowing for evaluation of portions of the collecting system where there is minimal contrast excretion as it does not limit information to only the highest attenuation voxels [5]. Although this method can have the disadvantage of being computationally costly (e.g., the algorithm is complex and requires a large amount of resources for execution), we find that it is worth the cost for the superior image quality and, because the urologists at our institution find them helpful, we routinely create VR reconstructions in our practice.

CPR, in contrast, does not take much computational power as it is simply the reformatting of images along the longitudinal axis of the upper urinary tract. In a study of 21 CTU cases at one institution, CPR alone did not result in increased sensitivity for detection of upper tract neoplasm as compared to axial images. However, combining CPR with axial images and coronal reformats increased sensitivity to over 90% as compared to sensitivities of 63-75% for any single image-type [28]. In a study of the utility of CPR in identification of ureteral obstruction in 60 patients, CPR was more sensitive (97.5%) for obstruction than MIP (75%) [29].

Dose reduction

In addition to dividing the contrast bolus and merging different post-contrast phases into a single acquisition, other techniques have been proposed to reduce the radiation dose in a CTU. The simplest method to reduce dose is to minimize scanner coverage. Given that dose is directly proportional to scan length, limiting coverage to the kidneys on the non-contrast phase and the kidneys through the bladder on nephrographic and excretory phase imaging achieves significant dose reduction without affecting imaging quality.

Scanning with reduced current or peak kilovoltage are additional options for reducing radiation dose. While these changes often come at the expense of increased image noise, this can be partially compensated for by iterative reconstruction and denoising techniques [13, 30, 31]. In addition, multiphase imaging offers the potential for dose reduction by selective reduction of dose in imaging phases that may

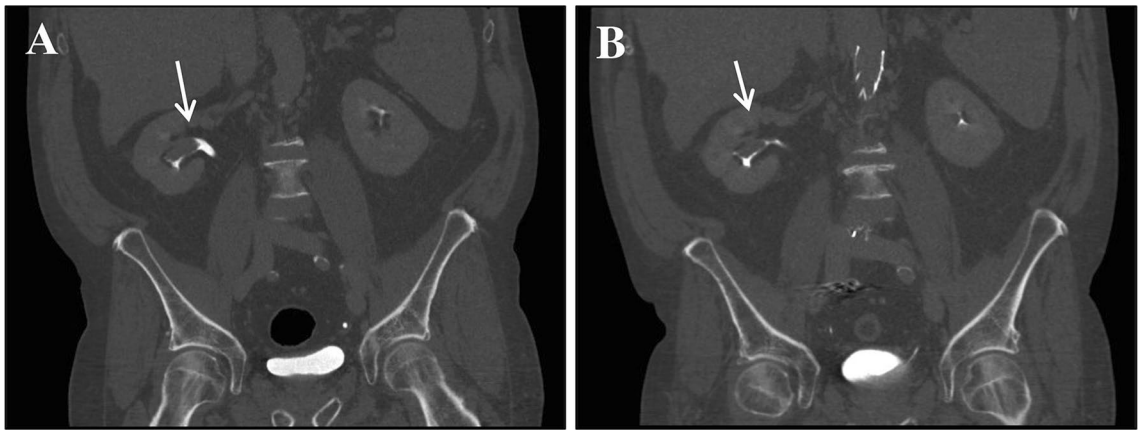

Fig. 7 Excretory phase imaging at different kVp. The excretory phase imaging of the same patient (a 72-year-old man with a BMI of 26.85) per original CT urogram protocol at 120 kVp (**a**) and at 100 kVp (**b**) after the implementation of the modified CT urogram protocol. Excretory phase imaging remains diagnostic and clearly demonstrates filling defect within the right renal pelvis (arrows), with a 22% dose reduction for this phase

tolerate higher levels of image noise while maintaining diagnostic confidence [32]. For CT urography, one potential strategy is to tolerate greater image noise for non-contrast and excretory phase imaging, while maintaining the highest image quality during the nephrographic phase.

Tube current is directly proportional to radiation dose [33]. If automated tube current modulation is being used, tube current may not be a fixed parameter but instead vary along the length of the patient. Depending on the vendor, optimizing the minimum and maximum tube currents (GE Healthcare scanners) or reference tube current–time product (Siemens Healthcare and Philips Healthcare scanners) and allowing more image noise (by increasing the noise index) for each phase of the scan may achieve incremental reductions in radiation dose without sacrificing diagnostic image quality [34, 35].

Tube potential can also be modulated to reduce dose. Decreasing tube voltage decreases the average photon energy. As the average photon energy approaches the k-edge of iodine, a greater proportion of interactions occur via the photoelectric effect. Thus, decreasing the tube voltage from 120 kVp (kilovoltage peak) to 80 kVp increases the attenuation of iodine by 70% [36]. Decreasing tube potential results in a nonlinear reduction in radiation dose. Compared with 80 kVp, radiation output is 1.5 times higher at 100 kVp and 2.5 times higher at 120 kVp [37]. As with most dose reduction techniques, this comes at the expense of increased image noise. However, resultant improvement in iodine-contrast may outweigh the increased noise, maintaining or potentially improving conspicuity of hypervascular or hypovascular lesions or ureteral irregularities [38, 39]. Decreasing the average photon energy may still prove problematic in obese patients where photon starvation can compromise image quality. However, in our experience, a tube potential of 100 kVp is sufficient to generate diagnostic quality images in the vast majority of adult patients (Fig. 7).

At our institution, we have successfully employed a combination of these changes within our CT urogram protocols (Fig. 8). Following review of existing methods, our updated protocol incorporated reductions in both minimum and maximum mA (milliamperes), as well as reduced scanner kVp in the excretory phase. Low kVp imaging was not applied to the non-contrast phase because of the need for accurate measurement of attenuation values (Hounsfield units) to assess for potential renal lesion enhancement in between the non-contrast and nephrographic phases. Reduction in tube potential increases measured Hounsfield values of all tissues relative to scans performed at higher kVp.

To prevent automated exposure control from increasing tube current when scanning at a lower kVp with automated exposure control, a concurrent increase in Noise Index (GE Healthcare) was required. A higher level of adaptive statistical iterative reconstruction (ASiR, GE Healthcare) was also used to help offset image noise. The combination of these simple techniques has successfully reduced average exam dose without compromising diagnostic quality of the exam.

Analysis of dose reports revealed that use of this low-dose protocol resulted in a decrease in mean effective dose of 30% compared to our previous protocol for patients over 40 (Figs. 7, 8). The total mean effective dose of the low-dose protocol was 13.2 mSv (median 11.8 mSv; range 9.8–19.5 mSv). The mean effective dose for the non-contrast phase was 2.9 mSv (median 2.8 mSv; range 2.4–4.2 mSv). The mean effective dose of the nephrographic phase was 5.8 mSv (median 5.3 mSv; range 4.4–8.3 mSv) and of the delayed phase was 4.5 mSv (median 3.8 mSv; range 3.1–6.9 mSv).

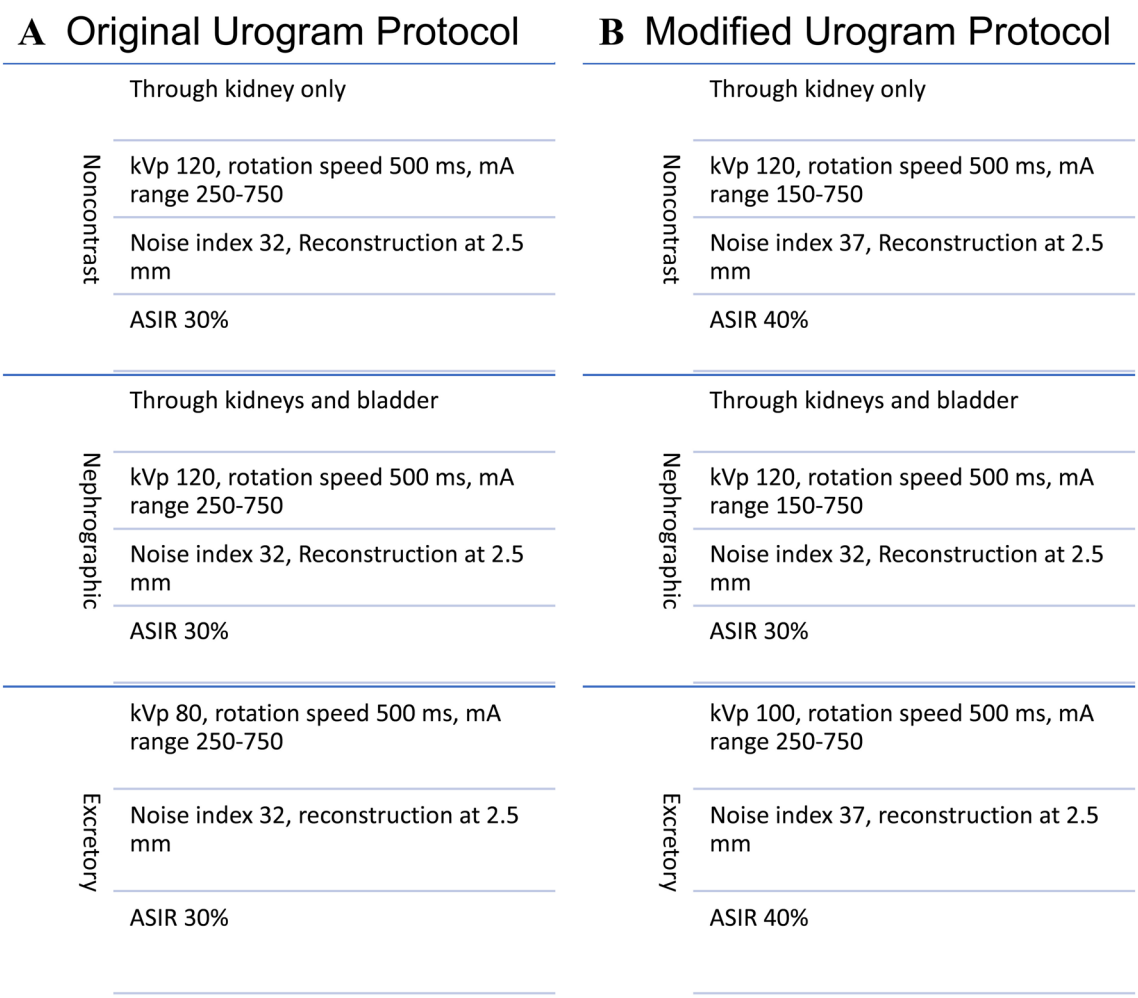

Fig. 8 CT Urogram protocol. The original CT Urogram protocol **a** for patients age > 40. Modified CT Urogram protocol incorporating dose reduction techniques **b** for patients age > 40

Using the split bolus protocol (for patients < 40 years of age) resulted in a further decrease in mean effective dose of 18% compared to our new low-dose protocol for patients over 40. The total mean effective dose of the split bolus protocol was 10.8 mSv (median 10.9 mSv; range 8.9–12.6 mSv). The mean effective dose for the non-contrast phase was 4.4 mSv (median 4.2 mSv; range 4.2–4.9 mSv). The mean effective dose of the combined nephrographic and delayed phase was 6.4 mSv (median 6.6 mSv; range 4.7–7.8 mSv).

Dual-energy CT has also emerged as a method for reducing radiation dose in CTU, as it allows for a creation of virtual non-enhanced images from a contrast-enhanced acquisition, eliminating the need for a separate non-contrast acquisition. High atomic number materials like iodine have a greater magnitude of change in attenuation between the low-energy and high-energy spectra as compared to low atomic number materials like calcium and water. Dual-energy CT algorithms utilize this feature of materials to quantify the amount of iodine in a tissue and to subtract iodine from contrast-enhanced images [40–43]. The reported accuracy for the characterization of renal mass contrast enhancement is as high as 94.6% with single-phase dual-source dual-energy CT [41]. However, the virtual non-enhanced images can be affected both by under-subtraction of dense contrast that mimics calculi, and by over-subtraction from algorithms seeking to compensate for possible under-subtraction [41]. This makes dual-energy CT less reliable in the characterization of smaller lesions less than 1.5 cm in size [43], and for small urinary calculi less than 2.5 mm in size [41]. Other reports have also described the utility of dual-energy CT in the diagnosis of urothelial tumors [44] and distinguishing bladder cancer from changes related to benign prostatic hyperplasia [45].

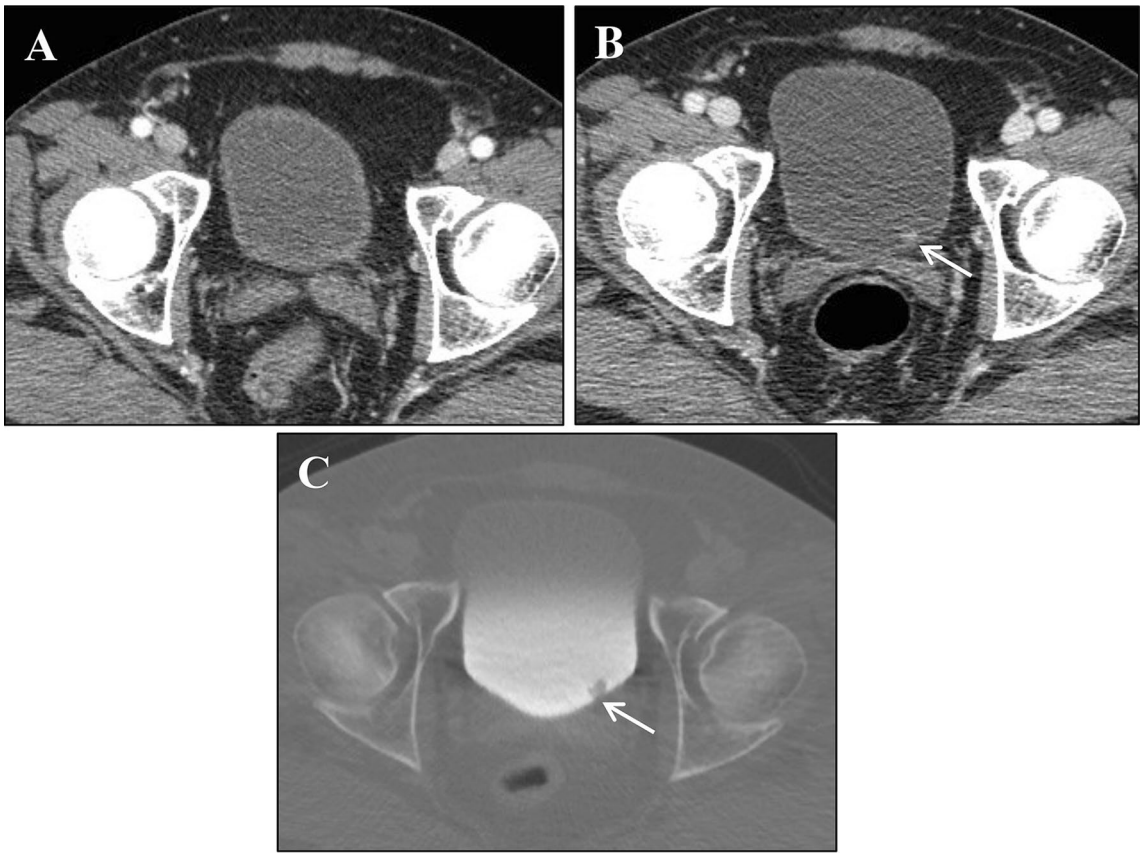

Fig. 9 Underdistension limits evaluation. A mucosal lesion is undetectable in axial images through the under-distended bladder (**a**). The lesion (arrows) becomes more visible with increasing bladder distension in axial images during both the nephrographic (**b**) and excretory (**c**) phases. Excretory phase is shown with the bone window setting for better visualization of the lesion within the contrast filled urinary bladder

Other ancillary techniques

Optimization of CTU protocol has also focused on improving distension and opacification of the ureters through ancillary techniques such as abdominal compression, prone positioning, oral and intravenous hydration, as well as diuretic administration.

Abdominal compression devices have been proposed to distend the upper tract. However, use of these devices can be rather burdensome since the technologist must remove the device after imaging the upper tract to allow urine and contrast to flow into the distal portions of the urinary tract. The distal urinary tract in the lower abdomen and pelvis must then be imaged in a separate acquisition. Furthermore, the devices are contraindicated in patients with other abdominal conditions such as abdominal aortic aneurysm, bowel obstruction, abdominal stomas, or recent abdominal surgery, and may not be effective in larger patients. Some authors suggest that they may not provide any added benefit in any patient, even the non-obese [46].

Prone positioning has similarly been suggested to improve distension of the upper tract by increasing dependent flow of contrast into the proximal portions of the collecting system. However, it is often uncomfortable for patients. Retrospective review of 114 CTU performed revealed that prone positioning only improved opacification of the anterior calyces and may in fact result in poorer overall collecting system distension as compared to supine positioning [47]. In light of the limited evidence supporting the utility of prone positioning and the potential for patient discomfort, we perform all imaging in the supine position.

Patient hydration, either with oral fluid administration or intravenous saline, may increase urine output, thereby increasing distension and opacification of the urinary tract and bladder [46, 48]. Adequate distension is critical in the visualization of subtle tumors, which may otherwise be undetectable (Fig. 9). Hydration does not significantly hinder workflow and is a relatively safe and easy ancillary technique to most CTU protocols. In our practice, the patient is encouraged to hydrate prior to the examination and is asked to consume up to 32 oz of water upon

arrival. We also give 250 mL normal saline intravenously following the administration of contrast bolus which has been shown to better opacify the distal ureters by increasing glomerular filtration rate [49]. Although some authors have subsequently debated whether intravenous saline truly improves ureteral opacification [50], others have shown that it at minimum improves proximal ureteral dilatation [46]. Additionally, we ask the patient to refrain from voiding 1 hour prior to the scan to optimize urinary bladder distension and opacification. We also instruct the patient to roll 360° immediately prior to excretory phase imaging to adequately mix contrast within the bladder.

Administration of a diuretic, usually intravenous Furosemide, has also been reported to increase urine flow rate and enhance urinary tract opacification and distension. However, Furosemide use has largely fallen out of favor due to the necessity of extra time and personnel to administer and evaluate the patient for medication allergies and possible hypotension.

Some institutions have also altered the type and volume of contrast in order to maximize ureteral distension. For example, using a larger volume of more dilute contrast (e.g. 200 mL Omnipaque 200 instead of the standard 100 to 120 mL Omnipaque 350) is proposed to increase excretion into the collecting system [5]. Using more dilute contrast also has the added advantage of reducing the likelihood of excessively dense contrast in the collecting system obscuring subtle urothelial thickening. On the other hand, dilute contrast may result in poor enhancement of the parenchymal organs, including the renal parenchyma, resulting in decreased sensitivity to identify solid organ pathologies such as renal cell carcinoma. In our experience, administration of slightly larger contrast volume and only mild dilution (e.g., 150 mL Omnipaque 300) reduces contrast density in the collecting system with better visualization through the less dense material and decreases possible streak artifacts. This slight optimization in contrast density potentially increases the sensitivity to identify subtle urothelial abnormalities. However, while Omnipaque 300 is preferred for the reasons stated above it is not readily available at our institution and Omnipaque 350 is used for CT urography chased by a saline bolus. Omnipaque 350 is the recommended injectable concentration of Omnipaque in most CT protocols, including CT angiography. Therefore, our institution chooses to stock only Omnipaque 350 in order to simplify the workflow for both the pharmacist and CT technologist.

Despite attempts to optimize CTU protocol, most institutions will occasionally have cases in which segments of the urinary tract are not opacified, most commonly the distal ureters. Some institutions will perform a repeat delayed scan limited to the non-opacified segments of the ureter. However, in a study of 59 male and 33 female patients, targeted delayed scanning did not result in the identification of any ureteral tumors, and increased radiation dose by an estimated 4.3 mSv per patient [51]. We do not routinely re-image non-opacified ureteral segments. We reserve additional imaging for cases where there is a specific concern, such as abnormal enhancement, mass, or associated upstream hydronephrosis.

Indication

CTU is most commonly used for the evaluation of hematuria due to its utility in the detection and characterization of many different pathologies, which affect the kidneys, urinary tract, and bladder.

Urothelial malignancies

Perhaps the major reason for the popularity of CTU in the evaluation of hematuria is the ability to detect upper tract urothelial malignancies that would not be detectable by other imaging modalities and cystoscopy. Though upper tract urothelial carcinoma accounts for only 5–10% of all urothelial tumors with an incidence of 1–2 cases per 100,000 individuals per year worldwide, the rate is increasing [52]. Upper tract urothelial malignancy is suggested by features such as urothelial thickening or enhancement, calcification, stricture, filling defect, mass, or upstream hydronephrosis. In one review of 27 pathology-proven upper tract urothelial carcinomas, 89% were detectable on CTU [53]. Though the sensitivity of CTU is high, not all positive exams will lead to a true urothelial carcinoma diagnosis. As a result of the relatively low prevalence of upper tract urothelial carcinoma compared to benign upper tract findings that mimic cancer such as blood clots or inflammatory ureteral thickening, studies report a low positive predictive value (53%) for upper tract malignancy diagnosis by CTU [54].

Unlike upper tract malignancies, which are poorly imaged by other techniques, urothelial malignancy of the bladder is easily imaged with cystoscopy, which is still the favored technique for detecting bladder malignancies. However, CTU has been reported to be up to 93% sensitive for urothelial carcinoma of the bladder and has the added advantage that distant metastases and lymphadenopathy can be identified on the same exam [55, 56]. Bladder malignancy is suggested on CTU by features such as focal mural hyperenhancement, thickening, a small nodule, or polypoid mass.

Meta-analysis of the published literature on CTU suggests that the pooled sensitivity for any urothelial malignancy was 96%, with a specificity of 99% [57].

Additionally, though not specifically designed for this purpose, CTU may also allow for the incidental detection of renal cell carcinomas, which will have higher attenuation

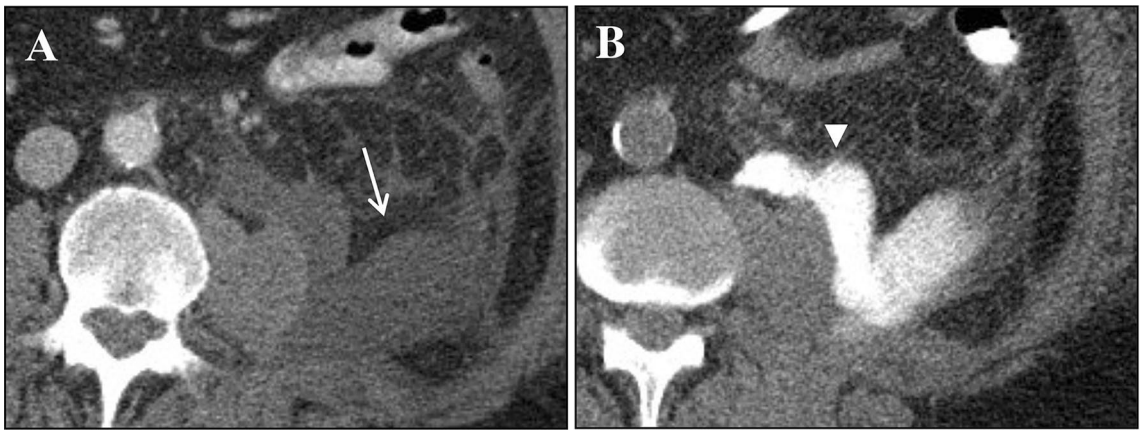

Fig. 10 Evaluation of urine leak. A 73-year-old male patient, one-week status post cystoprostatectomy for bladder cancer was evaluated with CTU with concern for a urine leak. A water attenuation collection (arrow) is seen on axial images in the non-contrast phase (**a**) and demonstrates progressive increase in attenuation (arrowhead) due to contrast-enhanced urine entering the collection on axial excretory phase imaging (**b**), consistent with a urine leak

than water on non-enhanced images and demonstrate enhancement on the nephrographic phase, typically greater than 20 HU [58].

Other pathologies detected on CTU

Although CTU is not typically indicated for the identification of urinary tract calculi as a non-contrast exam alone should be sufficient, calculi are frequently detected on CTU performed for the evaluation of asymptomatic hematuria. CTU can also identify benign inflammatory conditions of the kidney [40], congenital anomalies of the urinary tract [40, 59], renal papillary abnormalities [60, 61], traumatic urine leaks [62], and ureteral intramural hematomas [60]. Additionally, post-surgical complications following urologic surgeries such as ileal conduit or neobladder formation [60], as well as local and metastatic tumor recurrence can be examined by CTU (Fig. 10).

Conclusion

CTU is a powerful tool and a highly useful imaging technique that allows for the detection and characterization of both benign and malignant conditions involving the urinary tract. The utility of CTU is now widely recognized and has become the imaging of choice in the evaluation of asymptomatic hematuria. With its growing use, the radiation dose of CTU becomes a greater concern. As such, there have been a variety of proposed techniques to minimize the radiation dose while still providing optimal urinary tract distension and opacification. New and improving technologies, such as dual-energy CT, post-acquisition reconstruction and reformatting algorithms, and acceptance of increased noise on the unenhanced and excretory phases of the exam will allow for the maintenance of image quality at a reduced radiation cost to the patient.

Compliance with ethical standards

Conflict of interest The authors declare no conflicts of interest.

References

1. Davis R, Jones JS, Barocas DA, Castle EP, Lang EK, Leveillee RJ, et al. (2012) Diagnosis, Evaluation and Follow-up of Asymptomatic Microhematuria (AMH) in Adults (2012). American Urological Association. https://www.auanet.org/guidelines/asymptomatic-microhematuria-(2012-reviewed-for-currency-2016). Accessed 22 Dec 2018.
2. (1995) ACR Appropriateness Criteria: Hematuria. American College of Radiology. https://acsearch.acr.org/list. Accessed 22 Dec 2018.
3. Silverman SG, Leyendecker JR, Amis ES (2009) What Is the Current Role of CT Urography and MR Urography in the Evaluation of the Urinary Tract?. Radiology 250: 309–23
4. Cowan NC (2012) CT urography for hematuria. Nat Rev Urol 9: 218–26
5. Raman SP, Fishman EK (2017) Upper and Lower Tract Urothelial Imaging Using Computed Tomography Urography. Radiol Clin North 55:225–41.
6. Raman SP, Horton KM, Fishman EK (2013) MDCT Evaluation of Ureteral Tumors: Advantages of 3D Reconstruction and Volume Visualization. Am J Roentgenol 201:1239–47.
7. Kawashima A, Vrtiska TJ, LeRoy AJ, Hartman RP, McCollough CH, King BF (2004) CT Urography. RadioGraphics 24:S35–54.
8. Kopka L, Fischer U, Zoeller G, Schmidt C, Ringert RH, Grabbe E (1997) Dual-phase helical CT of the kidney: value of the corticomedullary and nephrographic phase for evaluation of renal lesions and preoperative staging of renal cell carcinoma. Am J Roentgenol 169:1573–8.

9. Helenius M, Dahlman P, Lonnemark M, Brekkan E, Wernroth L, Magnusson A (2016) Comparison of post contrast CT urography phases in bladder cancer detection. Eur Radiol 26:585–91.
10. Helenius M, Dahlman P, Magnusson M, Lönnemark M, Magnusson A (2014) Contrast enhancement in bladder tumors examined with CT urography using traditional scan phases. Acta Radiol 55:1129–36.
11. Joffe SA, Servaes S, Okon S, Horowitz M (2003) Multi–Detector Row CT Urography in the Evaluation of Hematuria. RadioGraphics 23:1441–55.
12. Takeuchi M, Konrad AJ, Kawashima A, Boorjian SA, Takahashi N (2015) CT Urography for Diagnosis of Upper Urinary Tract Urothelial Carcinoma: Are Both Nephrographic and Excretory Phases Necessary? Am J Roentgenol 205:W320–7.
13. Van Der Molen AJ, Cowan NC, Mueller-Lisse UG, Nolte-Ernsting CCA, Takahashi S, Cohan RH, et al. (2007) CT urography: definition, indications and techniques. A guideline for clinical practice. Eur Radiol 18:4.
14. Sheth S, Fishman EK (2004) Multi-Detector Row CT of the Kidneys and Urinary Tract: Techniques and Applications in the Diagnosis of Benign Diseases. RadioGraphics 24:e20–e20.
15. Akbar SA, Mortele KJ, Baeyens K, Kekelidze M, Silverman SG (2005) Multidetector CT urography: techniques, clinical applications, and pitfalls. Semin Ultrasound CT MRI 25:41–54.
16. Nolte-Ernsting C, Cowan N (2006) Understanding multislice CT urography techniques: many roads lead to Rome. Eur Radiol 16:2670–86.
17. Kemper J, Regier M, Stork A, Adam G, Nolte-ernsting C (2006) Improved Visualization of the Urinary Tract in Multidetector Ct Urography (mdctu): Analysis of Individual Acquisition Delay and Opacification Using Furosemide and Low-dose Test Images. J Comput Assist Tomogr 30:751–7.
18. Johnson PT, Horton KM, Fishman EK (2010) Optimizing Detectability of Renal Pathology With MDCT: Protocols, Pearls, and Pitfalls. Am J Roentgenol 194:1001–12.
19. Kupershmidt M, Margolis M, Jang H-J, Massey C, Metser U (2011) Evaluation of Upper Urinary Tract Tumors With Portal Venous Phase MDCT: A Case-Control Study. Am J Roentgenol 197:424–8.
20. Metser U, Goldstein MA, Chawla TP, Fleshner NE, Jacks LM, O'Malley ME (2012) Detection of Urothelial Tumors: Comparison of Urothelial Phase with Excretory Phase CT Urography—A Prospective Study. Radiology 264:110–8.
21. Lee D, Cho E-S, Kim JH, Kim YP, Lee H-K, Yu J-S, et al (2017) Optimization of Split-Bolus CT Urography: Effect of Differences in Allocation of Contrast Medium and Prolongation of Imaging Delay. Am J Roentgenol 209:W10–7.
22. Chow LC, Kwan SW, Olcott EW, Sommer G (2007) Split-Bolus MDCT Urography with Synchronous Nephrographic and Excretory Phase Enhancement. Am J Roentgenol 189:314–22.
23. Shaish H, Newhouse JH (2017) Split-bolus CT urogram: Is less more? Abdom Radiol. 42:2119–26.
24. Kekelidze M, Dwarkasing RS, Dijkshoorn ML, Sikorska K, Verhagen PCMS, Krestin GP (2010) Kidney and Urinary Tract Imaging: Triple-Bolus Multidetector CT Urography as a One-Stop Shop—Protocol Design, Opacification, and Image Quality Analysis. Radiology 255:508–16.
25. Jinzaki M, Kikuchi E, Akita H, Sugiura H, Shinmoto H, Oya M (2016) Role of computed tomography urography in the clinical evaluation of upper tract urothelial carcinoma. Int J Urol 23:284–98.
26. Dalrymple NC, Prasad SR, Freckleton MW, Chintapalli KN (2005) Introduction to the Language of Three-dimensional Imaging with Multidetector CT. RadioGraphics 25:1409–28.
27. Chow LC, Sommer FG (2001) Multidetector CT Urography with Abdominal Compression and Three-Dimensional Reconstruction. Am J Roentgenol 177:849–55.
28. Dillman JR, Caoili EM, Cohan RH, Ellis JH, Francis IR, Schipper MJ (2012) Detection of upper tract urothelial neoplasms: sensitivity of axial, coronal reformatted, and curved-planar reformatted image-types utilizing 16-row multi-detector CT urography. Abdom Imaging 33:707–16.
29. Shweel M, Abd-El Gawad EA, Abd-El Gawad EA, Fath El Bab TK (2012) Assessment of ureteric obstruction with 16-MDCT: Curved planar reformats versus three-dimensional volume-rendered images and their corresponding maximum intensity projections. Egypt J Radiol Nucl Med 43:623–30.
30. Page L, Wei W, Kundra V, Rong XJ (2016) Dose reduction in CT urography and vasculature phantom studies using model-based iterative reconstruction. J Appl Clin Med Phys 17:334–42.
31. Sagara Y, Hara AK, Pavlicek W, Silva AC, Paden RG, Wu Q (2010) Abdominal CT: Comparison of Low-Dose CT With Adaptive Statistical Iterative Reconstruction and Routine-Dose CT With Filtered Back Projection in 53 Patients. Am J Roentgenol 195:713–9.
32. Dahlman P, van der Molen AJ, Magnusson M, Magnusson A (2012) How Much Dose Can Be Saved in Three-Phase CT Urography? A Combination of Normal-Dose Corticomedullary Phase With Low-Dose Unenhanced and Excretory Phases. Am J Roentgenol 199:852–60.
33. Maldjian PD, Goldman AR (2013) Reducing Radiation Dose in Body CT: A Primer on Dose Metrics and Key CT Technical Parameters. Am J Roentgenol 200:741–7.
34. Mayo-Smith WW, Hara AK, Mahesh M, Sahani DV, Pavlicek W (2014) How I Do It: Managing Radiation Dose in CT. Radiology 273:657–72.
35. Hara AK, Welinitz CV, Paden RG, Pavlicek W and Sahani DV (2013) Reducing Body CT Radiation Dose: Beyond Just Changing the Numbers. Am J Roentgenol 201: 33-40.
36. Seyal AR, Arslanoglu A, Abboud SF, Sahin A, Horowitz JM, Yaghmai V (2015) CT of the Abdomen with Reduced Tube Voltage in Adults: A Practical Approach. RadioGraphics 35:1922–39.
37. Lira D, Padole A, Kalra MK, Singh S (2015) Tube Potential and CT Radiation Dose Optimization. Am J Roentgenol 204:W4–10.
38. Yu L, Fletcher JG, Grant KL, Carter RE, Hough DM, Barlow JM, et al. (2013) Automatic Selection of Tube Potential for Radiation Dose Reduction in Vascular and Contrast-Enhanced Abdominopelvic CT. Am J Roentgenol 201:W297–306.
39. Macari M, Spieler B, Kim D, Graser A, Megibow AJ, Babb J, et al. (2010) Dual-Source Dual-Energy MDCT of Pancreatic Adenocarcinoma: Initial Observations With Data Generated at 80 kVp and at Simulated Weighted-Average 120 kVp. Am J Roentgenol 194:W27–32.
40. Potenta SE, D'Agostino R, Sternberg KM, Tatsumi K, Perusse K (2015) CT Urography for Evaluation of the Ureter. RadioGraphics 35: 709-26.
41. Kaza RK, Platt JF. Renal applications of dual-energy CT (2016) Abdom Radiol 41:1122–32.
42. Kaza RK, Platt JF, Megibow AJ (2013) Dual-energy CT of the urinary tract. Abdom Imaging 38:167–79.
43. Kaza RK, Ananthakrishnan L, Kambadakone A, Platt JF (2017) Update of Dual-Energy CT Applications in the Genitourinary Tract. Am J Roentgenol 208:1185–92.
44. Hansen C, Becker CD, Montet X, Botsikas D (2014) Diagnosis of Urothelial Tumors With a Dedicated Dual-Source Dual-Energy MDCT Protocol: Preliminary Results. Am J Roentgenol 202:W357–64.
45. Chen A, Liu A, Liu J, Tian S, Wang H, Liu Y (2016) Application of dual-energy spectral CT imaging in differential diagnosis of

bladder cancer and benign prostate hyperplasia. Medicine (Baltimore) 95: e5705.
46. Caoili EM, Inampudi P, Cohan RH, Ellis JH (2005) Optimization of Multi–Detector Row CT Urography: Effect of Compression, Saline Administration, and Prolongation of Acquisition Delay. Radiology 235:116–23.
47. Wang ZJ, Coakley FV, Joe BN, Qayyum A, Meng MV, Yeh BM (2009) Multidetector row CT urography: does supine or prone positioning produce better pelvecalyceal and ureteral opacification? Clin Imaging 33:369–73.
48. Szolar DH, Tillich M, Preidler KW (2010) Multi-detector CT urography: effect of oral hydration and contrast medium volume on renal parenchymal enhancement and urinary tract opacification—a quantitative and qualitative analysis. Eur Radiol. 20:2146–52.
49. McTavish JD, Jinzaki M, Zou KH, Nawfel RD, Silverman SG (2002) Multi–Detector Row CT Urography: Comparison of Strategies for Depicting the Normal Urinary Collecting System. Radiology 225:783–90.
50. Sudakoff GS, Dunn DP, Hellman RS, Laguna MA, Wilson CR, Prost RW, et al (2006) Opacification of the Genitourinary Collecting System During MDCT Urography with Enhanced CT Digital Radiography: Nonsaline Versus Saline Bolus. Am J Roentgenol. 186:122–9.
51. Hack K, Pinto PA, Gollub MJ (2012) Targeted Delayed Scanning at CT Urography: A Worthwhile Use of Radiation? Radiology 265:143–50.
52. Soria F, Shariat SF, Lerner SP, Fritsche H-M, Rink M, Kassouf W, et al (2017) Epidemiology, diagnosis, preoperative evaluation and prognostic assessment of upper-tract urothelial carcinoma (UTUC). World J Urol. 35:379–87.
53. Caoili EM, Cohan RH, Inampudi P, Ellis JH, Shah RB, Faerber GJ, et al. (2005) MDCT Urography of Upper Tract Urothelial Neoplasms. Am J Roentgenol. 184:1873–81.
54. Sadow CA, Wheeler SC, Kim J, Ohno-Machado L, Silverman SG (2010) Positive Predictive Value of CT Urography in the Evaluation of Upper Tract Urothelial Cancer. Am J Roentgenol. 195:W337–43.
55. Raman SP, Fishman EK (2014) Bladder Malignancies on CT: The Underrated Role of CT in Diagnosis. Am J Roentgenol 203:347–54.
56. Hartman R, Kawashima A (2017) Lower tract neoplasm: Update of imaging evaluation. Eur J Radiol. 97:119–30.
57. Chlapoutakis K, Theocharopoulos N, Yarmenitis S, Damilakis J (2010) Performance of computed tomographic urography in diagnosis of upper urinary tract urothelial carcinoma, in patients presenting with hematuria: Systematic review and meta-analysis. Eur J Radiol 73:334–8.
58. O'Connor OJ, Maher MM (2010) CT Urography. Am J Roentgenol. 195:W320–4.
59. Surabhi VR, Menias CO, George V, Matta E, Kaza RK, Hasapes J (2015) MDCT and MR Urogram Spectrum of Congenital Anomalies of the Kidney and Urinary Tract Diagnosed in Adulthood. Am J Roentgenol. 205:W294–304.
60. Kawamoto S, Duggan P, Sheth S, Miyamoto H, Kazi ZN, Fishman EK (2017) Renal Papillary and Calyceal Lesions at CT Urography: Genitourinary Imaging. RadioGraphics 37:358–9.
61. Alderson SM, Hilton S, Papnicolaou N (2011) CT urography: Review of technique and spectrum of diseases. Appl Radiol. 40:6–13.
62. Dane B, Baxter AB, Bernstein MP (2017) Imaging Genitourinary Trauma. Radiol Clin North Am 55:321–35.